Bioorg. Med. Chem. 30 (2021) 115927

Contents lists available at ScienceDirect

Bioorganic & Medicinal Chemistry

journal homepage: www.elsevier.com/locate/bmc

Novel indolylarylsulfone derivatives as covalent HIV-1 reverse transcriptase inhibitors specifically targeting the drug-resistant mutant Y181C

Ping Gao [a,1], Shu Song [a,1], Estrella Frutos-Beltrán [b,1], Wenxin Li [a], Bin Sun [c], Dongwei Kang [a], Jinmi Zou [a], Jian Zhang [a], Christophe Pannecouque [d], Erik De Clercq [d], Luis Menéndez-Arias [b,*], Peng Zhan [a,*], Xinyong Liu [a,*]

[a] Department of Medicinal Chemistry, Key Laboratory of Chemical Biology, Ministry of Education, School of Pharmaceutical Sciences, Shandong University, Ji'nan 250012, PR China
[b] Centro de Biología Molecular "Severo Ochoa" (Consejo Superior de Investigaciones Científicas & Universidad Autónoma de Madrid), Madrid, Spain
[c] Institute of BioPharmaceutical Research, Liaocheng University, 1 Hunan Road, Liaocheng 252000, PR China
[d] Rega Institute for Medical Research, K. U. Leuven, Minderbroedersstraat 10, B-3000 Leuven, Belgium

ARTICLE INFO

Keywords:
HIV-1
Indolylarylsulfones
NNRTIs
Y181C
Covalent inhibitor

ABSTRACT

Non-nucleoside reverse transcriptase inhibitors (NNRTIs) are widely used in combination therapies against HIV-1. However, emergent and transmitted drug resistance compromise their efficacy in the clinical setting. Y181C is selected in patients receiving nevirapine, etravirine and rilpivirine, and together with K103N is the most prevalent NNRTI-associated mutation in HIV-infected patients. Herein, we report on the design, synthesis and biological evaluation of a novel series of indolylarylsulfones bearing acrylamide or ethylene sulfonamide reactive groups as warheads to inactivate Cys181-containing HIV-1 RT via a Michael addition reaction. Compounds **I-7** and **I-9** demonstrated higher selectivity towards the Y181C mutant than against the wild-type RT, in nucleotide incorporation inhibition assays. The larger size of the NNRTI binding pocket in the mutant enzyme facilitates a better fit for the active compounds, while stacking interactions with Phe227 and Pro236 contribute to inhibitor binding. Mass spectrometry data were consistent with the covalent modification of the RT, although off-target reactivity constitutes a major limitation for further development of the described inhibitors.

1. Introduction

The global pandemic of human immunodeficiency virus type 1 (HIV-1) remains as a major threat to human health worldwide.[1] Standard treatments against HIV-1 infection, including highly active antiretroviral therapies (HAART), often combine drugs targeting the three viral enzymes: protease, reverse transcriptase (RT) and integrase, among which RT has become the primary target for anti-HIV chemotherapy.[2] However, emergent and transmitted drug resistance hamper the effectiveness of antiretroviral therapies.[3]

K103N and Y181C are the most common mutations associated with resistance to non-nucleoside RT inhibitors (NNRTIs) and several studies have shown that their prevalence in NNRTI-resistant viruses can be as high as 40–60% for K103N, and 15–25% for Y181C.[4,5] Recent studies have also shown an increased prevalence of those mutations among transmitted drug-resistant viruses in different regions of the world, most notably Sub-Saharan Africa and Latin America.[6,7]

Although Y181C has been usually associated with high-level resistance to nevirapine (a first generation NNRTI), this amino acid substitution can be selected *in vivo* after exposure to etravirine or rilpivirine, while conferring 3- to 5-fold reduced susceptibility to those drugs in phenotypic assays (reviewed in Refs.[3,5]). Many efforts in antiretroviral therapy have been focused on the possibility of blocking replication of HIV strains carrying the Y181C substitution in their RT. An attractive approach involves the covalent modification of the enzyme through targeting Cys181. Recently, Chan *et al.*[8] described 2-naphthyl phenyl ether derivatives containing α-halo amide and acrylamide warheads that eliminated the activity of Cys181-containing HIV-1 RT. These

* Corresponding authors.
E-mail addresses: lmenendez@cbm.csic.es (L. Menéndez-Arias), zhanpeng1982@sdu.edu.cn (P. Zhan), xinyongl@sdu.edu.cn (X. Liu).
[1] These authors contributed equally to this work.

https://doi.org/10.1016/j.bmc.2020.115927
Received 25 April 2020; Received in revised form 1 December 2020; Accepted 2 December 2020
Available online 10 December 2020

compounds showed similar efficacy against the wild-type (WT) RT in *in vitro* assays, with IC_{50}s in the low micromolar range.

In this report, we have used indolylarylsulfones to develop new covalent inhibitors targeting Cys181 in HIV-1 RT. Indolylarylsulfone derivatives constitute a potent class of NNRTIs developed from the Merck prototype compound L-737,126[9] (Fig. 1). Derivatives of this molecule have shown inhibitory activities against the WT virus in the nanomolar range[10] (reviewed in[11]). Crystallography and molecular studies based on the complex of HIV-1 RT and the indolylarylsulfone derivative **7e** (Fig. 1) showed that the saturated pyrrole ring locates at the hydrophobic pocket lined by residues Tyr181, Tyr188, Phe227 and Tyr318.[12] The antiviral activity of sulfonamide **7e** was similar to that previously reported for L-737,126.[9,12] Assuming the location of the saturated pyrrol ring close to position 181, we predicted that the introduction of a reactive group through a Michael reaction would facilitate the formation of a covalent bond with the mutated cysteine thereby blocking the activity of the Y181C mutant RT.

Acrylamide and ethylene sulfonamide "warheads" were introduced to explore the possibility of obtaining covalently modified Y181C RTs. Indolylarylsulfone derivatives containing rings of different sizes (five- and six-membered) were synthesized and tested in enzymatic and cell-based assays to explore structure diversity and potential improvements in their inhibition capacity. Our results show the specific inhibition of the HIV-1 RT mutant Y181C through covalent modification of the enzyme using indolylarylsulfone derivatives, but underline limitations caused by off-target covalent binding that may result in relatively high cytotoxicity.

2. Results and discussion

2.1. Chemistry

The synthetic routes of novel indolylarylsulfone derivatives are outlined in Scheme 1. Target compounds were synthesized from the commercially available starting material ethyl 5-bromoindole-2-carboxylate (**1**). First, compound **1** was reacted with concentrated sulfuric acid in acetic anhydride solution to obtain intermediate 5-bromo-2-ethyl ester-1H-indole-3-sulfonic acid (**2**). Then, further reaction with oxalyl chloride in dichloromethane and a catalytic amount of dimethylformamide led to the synthesis of ethyl 5-bromo-3-(chlorosulfonyl)-1H-indole-2-carboxylate (**3**). Compound **3** reacted with different amino substituents to generate the compounds of series **4**. Then, these molecules were esterified into amides (under ammonia gas) to form the **5** series of intermediates. Finally, the *t*-butyloxycarboryl group was removed under trifluoroacetic acid, and the exposed amino groups were acylated with acryloyl chloride or ethylenesulfonyl chloride to obtain the target compounds.

2.2. Biological activity

2.2.1. Antiviral activity in cell culture and HIV-1 RT inhibition assays

The synthesized indolylarylsulfones were first evaluated in cell culture assays for their anti-HIV activity against WT HIV-1 and HIV-2 strains (IIIB and ROD, respectively). Efavirenz and compound **7e** were used as positive controls. As shown in Fig. 2, most of the compounds were inactive and showed relatively high cytotoxicity, although some inhibition was observed with compounds **I-3** and **I-7**. The most potent derivative was **I-7** and showed an IC_{50} of 9.74 ± 0.34 μM against WT HIV-1. No inhibition was observed with any of the tested compounds when tested against WT HIV-2 ROD (data not shown).

The structure-activity relationship (SAR) analysis based on the results of the antiviral assays showed that the compounds with the ethylene sulfonamide substitution all exhibited higher cytotoxicity than those with acrylamide warheads, indicating that ethylene sulfonamide is potentially more toxic. As to the acrylamide substitution series (compounds **I-1** to **I-5**), SAR analysis reveals that: (i) the lowest toxicitity (highest CC_{50}) is shown by the six-membered ring-substituted compound **I-3** that lacks a chiral center; (ii) if the acrylamide reactive group is attached to a chiral carbon atom, the compound is more toxic when the C atom is in the *S* configuration (CC_{50}: **I-2** > **I-4**, **I-5**); and (iii) for compounds without the ethylene sulfonamide warhead (**I-1** to **I-5**), higher toxicities were shown by molecules containing an extended sulfonamide linker between the two rings (CC_{50}: **I-1, I-3** > **I-2, I-4**, **I-5**).

In contrast, in the series containing the ethylene sulfonamide warhead (compounds **I-6** to **I-9**), longer linkers due to the presence of an amide between the sulfonyl group and the piperidine and pyrrolidine rings, as in compounds **I-7** and **I-9**, reduced their toxicity in comparison to **I-6** and **I-8**.

Despite the cytotoxicity and weak inhibitory activity of all tested compounds in cell culture assays, we also determined their inhibitory potential in nucleotide incorporation assays carried out with heteropolymeric template-primers. In agreement with the results of the cell culture experiments, none of the indolylarylsulfone derivatives showed significant activity against WT HIV-1 RT (BH10 RT) at 100 μM (Fig. 3).

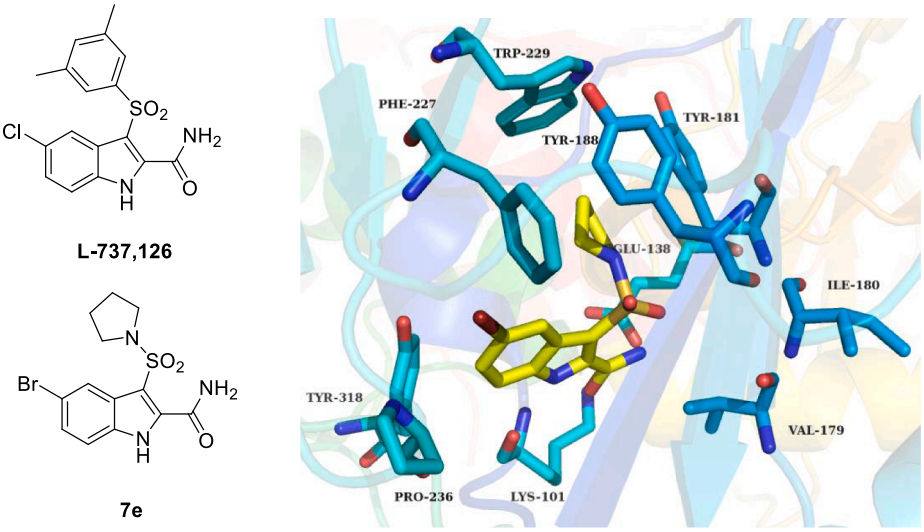

Fig. 1. Indolylarylsulfone derivatives and schematic diagram showing the location of compound **7e** within the NNRTI binding pocket of HIV-1 RT. Compound **7e** (yellow) and amino acid side chains in the binding pocket (blue) are shown using a stick representation. The figure was generated with the PyMol software (www.pymol.org). Coordinates were taken from the Protein Data Bank (file 2RF2)[12].

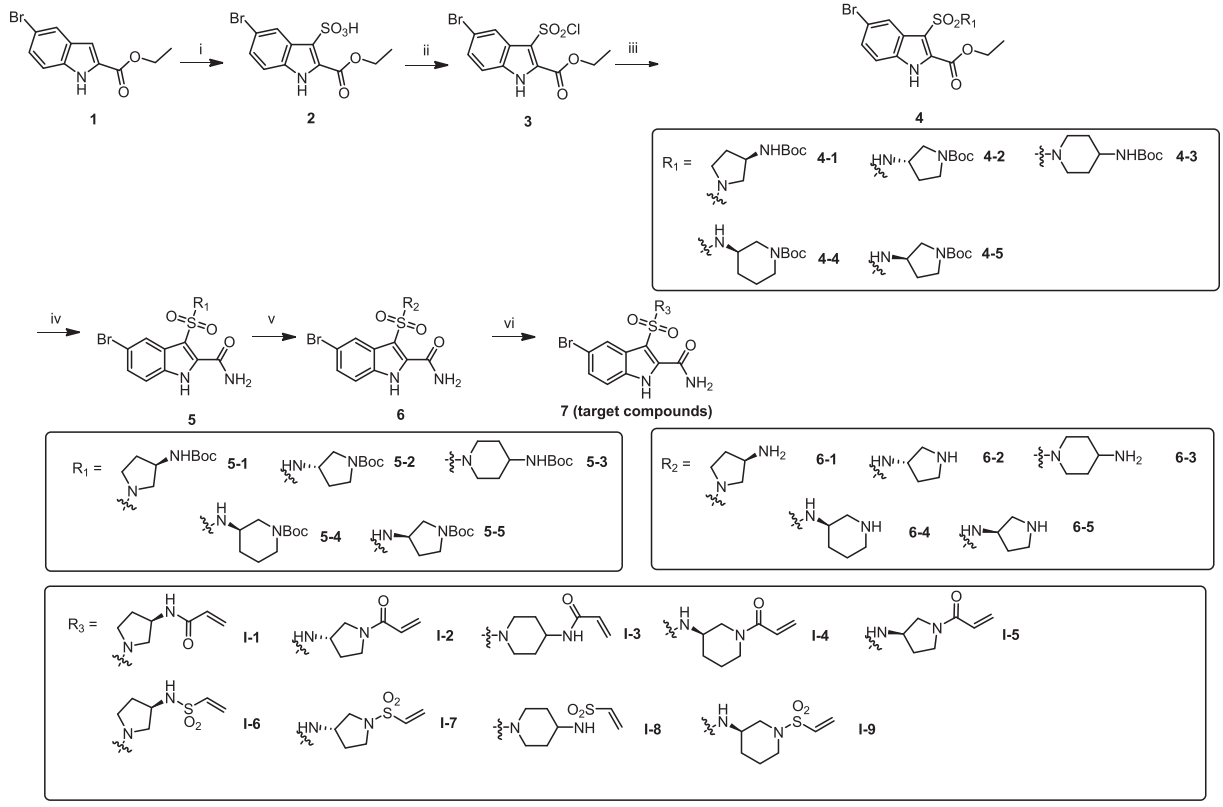

Scheme 1. Reagents and conditions: (i) H_2SO_4, acetic anhydride, r.t., 15 h. (ii) oxalyl chloride, DMF, DCM, reflux, 3 h. (iii) substituted alkylamine, DCM, Et_3N, r.t., overnight. (iv) NH_3, CH_3OH, 70 °C, overnight. (v) TFA, DCM, r.t., overnight. (vi) acryloyl chloride or 2-chloroethanesulfonyl chloride, THF, Et_3N, 12 h.

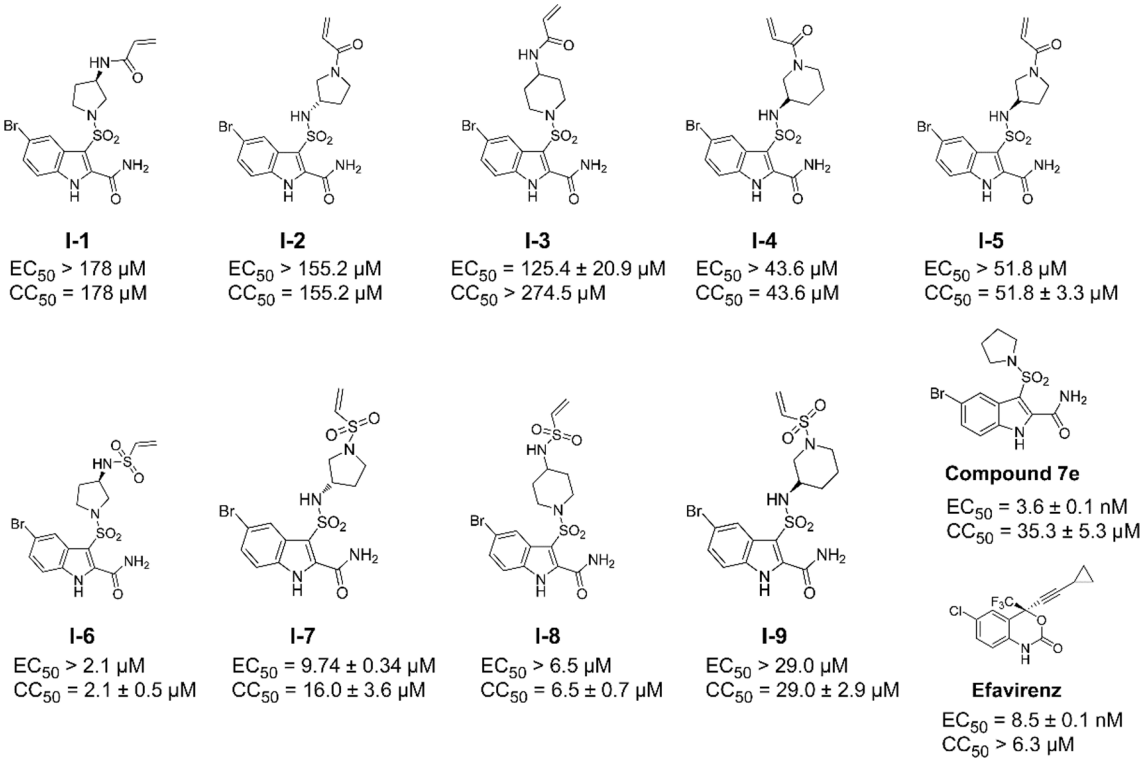

Fig. 2. Antiviral activity against the WT HIV-1 IIIB strain of indolylarylsulfone derivatives in MT-4 cell culture assays. EC_{50} indicates the concentration of compound required to achieve 50% protection against HIV-1-induced cytotoxicity, as determined by the MTT method. CC_{50} is the concentration required to reduce the viability of mock-infected cell cultures by 50%, as determined by the MTT method.

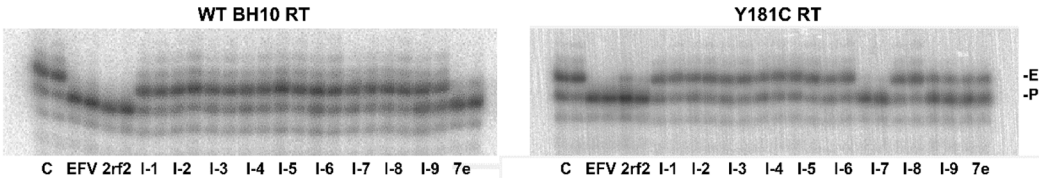

Fig. 3. Nucleotide incorporation assays carried out with WT and mutant RTs. Assays were carried out with template-primer D38/[^{32}P]25PGA. Enzyme and template-primer were supplied at 12 and 30 nM, respectively. The incorporation reaction was carried out at 37 °C in the presence of inhibitor and dTTP at 100 μM each. Aliquots were taken after 15 and 30 s. C shows control experiments carried out in the absence of inhibitor. P and E indicate the position of the labeled primer (25PGA), and the extended product after the incorporation of dTTP, respectively. 2rf2 stands for compound L-737126.

However, **I-7** showed potent inhibitory activity against mutant Y181C RT. Efavirenz, L-737,126 (5-bromo-3-(pyrrolidin-1-ylsulfonyl)-1H-indole-2-carboxamide; 2rf2) and compound 7e[9,12] used as controls, were effective inhibitors of both WT and Y181C RTs, although L-737,126 and 7e were less effective against Y181C (Fig. 3).

Compounds **I-7** and **I-9** showed the largest inhibitory effect against Y181C RT in single nucleotide incorporation assays (Fig. 3). Their 50% inhibitory concentrations (IC_{50}s) against WT HIV-1_{BH10} RT and mutant Y181C are shown in Table 1. In these experiments, efavirenz and compound 7e were used as controls and were found to be active against both enzymes, although the inhibitory capacity of compound 7e was reduced by >100-fold in the case of mutant Y181C, in agreement with previous reports showing its lower efficacy in antiviral assays against the mutant virus.[12] HPLC analysis showed that after a 24-hour incubation at pH 2.0 and 7.4 (in phosphate buffer), **I-7** remained stable, showing the same mobility than at time 0, and retaining more than 95% peak intensity after reverse-phase chromatography.

I-7 and **I-9** failed to inhibit the WT RT at concentrations as high as 100 μM. However, both compounds inhibited the mutant Y181C RT with IC_{50} values of 18.2 ± 4.1 μM and 75.2 ± 8.9 μM for **I-7** and **I-9**, respectively. Their inhibitory activity was not largely affected by dithiothreitol (DTT), although **I-7** showed higher potency when DTT was excluded from the reaction mixture (IC_{50} = 11.3 ± 2.09 μM). All the nucleotide incorporation reactions were carried out after pre-incubating the enzyme with the inhibitor for 5 min at 37 °C. However, in the absence of DTT, when the incubation time was extended to 60 min, the IC_{50} value for **I-7** against Y181C RT decreased to 2.26 ± 0.68 μM.

The antiviral activity of **I-7** and **I-9** was also tested in cell culture against WT and mutant HIV-1 IIIB strains, in an experiment carried out independently from those reported in Fig. 2. As shown in Table 2, both compounds showed some activity against the mutant virus, although with relatively low selectivity indexes (9.3 and 7.7, for **I-7** and **I-9**, respectively) due to the cytotoxicity of those compounds. Despite these limitations, **I-7** shows measurable antiviral activity by targeting Cys181 in the HIV-1 NNRTI binding site.

Table 1
Inhibitory activity of selected compounds in nucleotide incorporation assays.

Compounds	IC_{50} (μM)		
	WT BH10	Y181C RT	
	Standard conditions	Standard conditions	Without DTT
I-7	>100 *	18.2 ± 4.1	11.3 ± 2.1
I-9	>100 *	75.2 ± 8.9	79.9 ± 15.0
Compound 7e	0.48 ± 0.09	59.0 ± 8.1	ND
Efavirenz	0.18 ± 0.01	0.24 ± 0.02	ND

* Less than 5% inhibition at 100 μM concentration of the inhibitor. ND, not determined.

Table 2
Activity against WT and mutant HIV-1 IIIB strains and cytotoxicity in MT-4 cells.

Compounds	EC_{50} (μM) [a]		CC_{50} (μM) [b]
	WT	Y181C	
I-7	9.74 ± 0.34	2.36 ± 0.91	22.0 ± 8.6
I-9	> 40.7	5.32 ± 1.02	40.7 ± 17.4
Etravirine	0.01 ± 0.001	ND [c]	ND
Rilpivirine	0.01 ± 0.001	ND	ND

[a] EC_{50}: concentration of compound required to achieve 50% protection of MT-4 cell cultures against HIV-1-induced cytotoxicity, as determined by the MTT method.
[b] CC_{50}: concentration required to reduce the viability of mock-infected cell cultures by 50%, as determined by the MTT method.
[c] Not determined.

2.2.2. *Mass spectrometry*

The molecular weights of complexes of **I-7** and Y181C HIV-1 RT were determined by matrix-assisted laser desorption/ionization-time of flight (MALDI-TOF) mass spectrometry. In these experiments the mutant Y181C RT (at around 30 μM) was incubated for 1 h at room temperature in the presence of **I-7** at concentrations as high as 1.3 mM. The results shown in Fig. 4 are consistent with the formation of covalent complexes when the mutant enzyme is incubated with the inhibitor. Peaks at *m/z* values of 65,947 and 51,634 were observed in determinations made with the mutant RT alone and correspond to subunits p66 and p51, respectively (Fig. 4A). Peaks of 33,056 and 25,868 are consistent with the expected two-fold mass-to-charge reduction. In contrast, at high concentrations of the inhibitor (i.e., 1.3 mM), peaks shifted to 66,714–67,126 Da for p66 and 52,244 for p51 (Fig. 4C). These mass increases were consistent with the incorporation of 2–3 indolylarylsulfones in p66 and 2 in p51. Each Y181C RT subunit contains three cysteine residues (Cys38, Cys181 and Cys280). Interestingly, in assays carried out with 50 μM **I-7**, we observed that the molecular mass of p51 remained unaffected (51,529 Da), although an increase of 364 Da was observed in p66 (molecular mass 66,311 Da) (Fig. 4B). These results were compatible with the covalent modification of Cys181 in NNRTI binding site of the Y181C mutant. In addition, the likely modification of additional Cys residues in the RT when higher concentrations of **I-7** are used is consistent with its relatively high cytotoxicity, which seems to be prone to off-target labeling of viral and cellular proteins.

Covalent modification of Cys181 was further demonstrated after trypsin digestion of the treated Y181C RT, and subsequent analysis by liquid chromatography-electrospray ionization tandem mass spectrometry (LC-ESI MS/MS). Before trypsin hydrolysis, cysteine residues were blocked with chloroacetamide. The LC-ESI MS/MS analysis of the Y181C RT treated with **I-7** for 1 h at 50 μM revealed the presence of a tryptic peptide QNPDIVICQYMDDLYVGSDLEIGQHRW with an expected molecular mass of 3496.39 Da, consistent with the presence of **I-7** (477.35

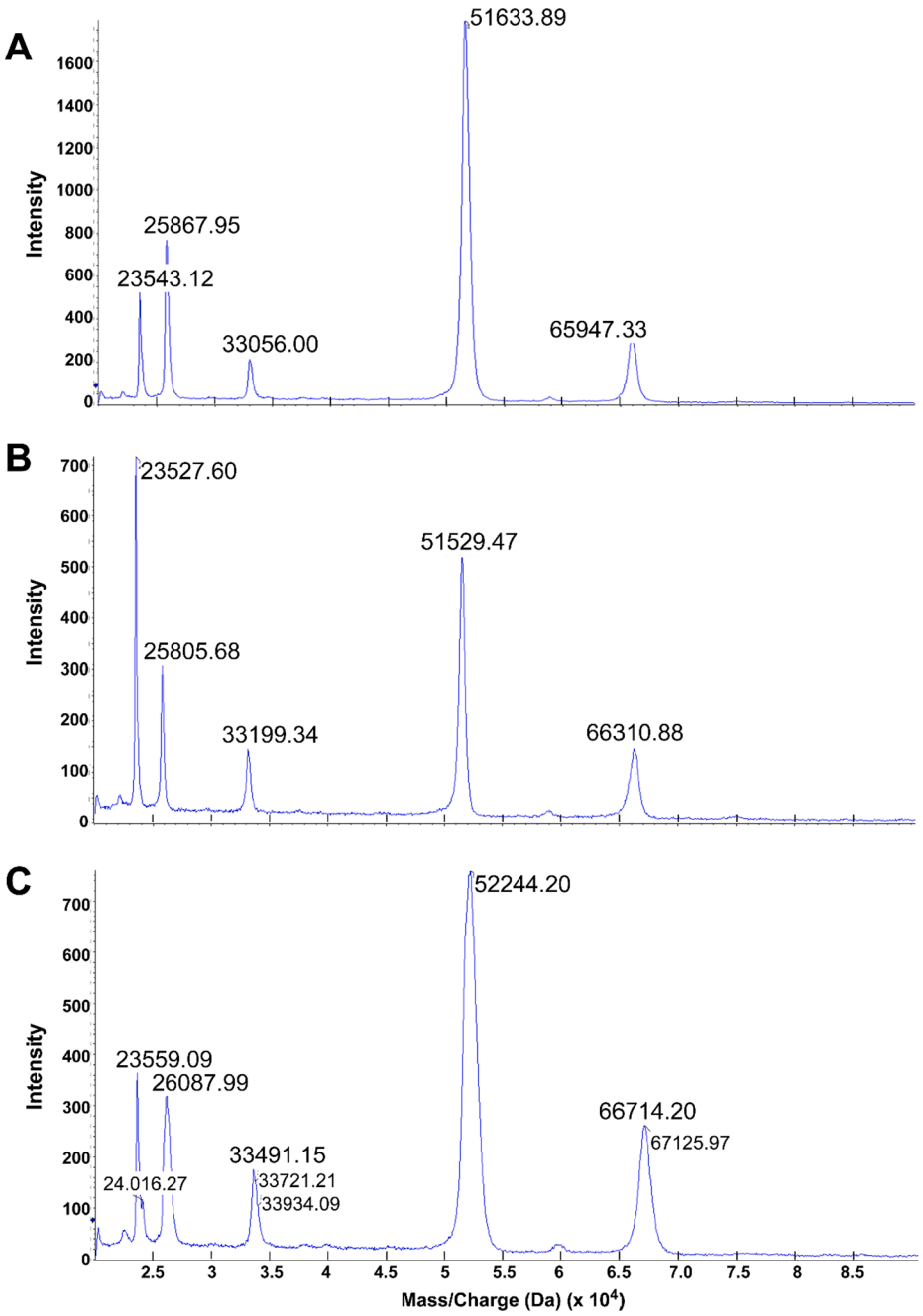

Fig. 4. Molecular weight determinations using MALDI-TOF mass spectrometry. (A) Y181C RT (without inhibitor). (B) Y181C RT incubated in the presence of **I-7** (50 μM). (C) Y181C RT incubated in the presence of **I-7** (1.3 mM).

Da) bound to Cys181 (Fig. 5A). In the same sample, we detected a carbamidomethylated derivative of the Cys-containing peptide with a molecular mass of 3077.42 Da. For all modified peptides, scores were relatively high and significant (Fig. 5A). The protein sequence coverages obtained with treated and untreated Y181C RTs were 82 and 83%, respectively, and all Cys-containing peptides were identified in the analysis (Supplementary Tables S1 and S2). However, the peptide of 3496.39 Da mentioned above was the only one identified whose molecular mass was consistent with the presence of **I-7** bound to Cys181. The identification of this covalently-modified peptide was further supported by MS/MS fragmentation patterns leading to the recognition of the internal sequence DDLYVGSDLEIG (Fig. 5B).

2.2.3. Molecular modeling

In order to gain further insight into the preferred binding mode of the tested compounds and rationalize results of the SAR analysis, molecular models of **I-7** bound to WT and Y181C mutant HIV-1 RT were obtained. According to the model of the Y181C mutant, stabilization of **I-7** in the NNRTI binding pocket can be achieved through interactions with the side chains of Phe227 and Pro236, as well as a hydrogen bond between the sulfone group of **I-7** and Lys101 (Fig. 6). The predicted conformation of **I-7** is compatible with the formation of a covalent bond between the ethylene sulfonamide reactive group and the side chain of Cys181, explaining the superior activity of **I-7** against the Y181C RT as compared with the WT enzyme. As for the binding mode of **I-7** in the WT RT, Fig. 6C shows the results of the docking experiment showing the highest-score model predicted by the molecular modeling software. As

A

Residues	Observed	Mr (expt)	Mr (calc)	ppm	M	Score	Expect	Peptide
170-202	984.245	3932.951	3932.944	1.76	2	40	0.0001	K.ILEPFKKQNPDIVICQYMDDLYVGSDLEIGQHR.T + Carbamidomethyl (C)
176-202	802.388	3205.525	3205.517	2.29	1	51	8.2e-06	K.KQNPDIVICQYMDDLYVGSDLEIGQHR.T + Carbamidomethyl (C)
177-202	770.361	3077.414	3077.422	-2.80	0	103	5e-11	K.QNPDIVICQYMDDLYVGSDLEIGQHR.T + Carbamidomethyl (C)
177-202	1026.815	3077.424	3077.422	0.61	0	129	1.2e-13	K.QNPDIVICQYMDDLYVGSDLEIGQHR.T + Carbamidomethyl (C)
177-202	1166.471	3496.391	3496.383	2.34	0	54	3.7e-06	K.QNPDIVICQYMDDLYVGSDLEIGQHR.T + I-7 (C) [Covalent modification]

B

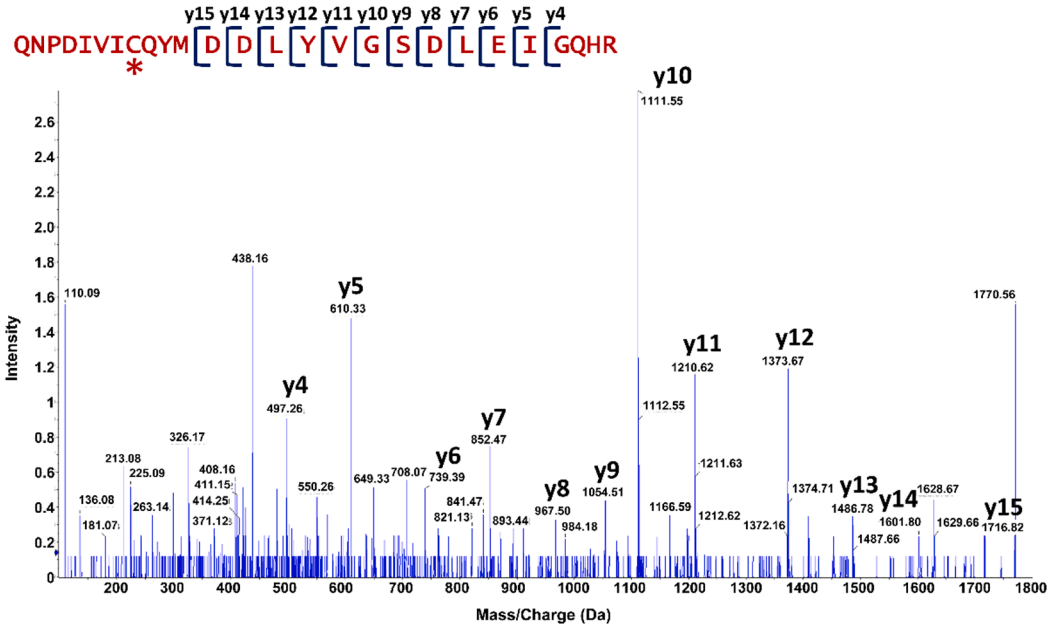

Fig. 5. Covalent modification of Cys181 by I-7. (A) Mascot software analysis of LC-ESI MS/MS data obtained for the Y181C RT mutant after treatment with **I-7** for 1 h at 50 μM, followed by blocking of available Cys residues with chloroacetamide. Modified Cys-containing peptides are shown. Peptide numbering is shifted three residues due to the addition of three residues (MNS) at the *N*-terminus of the recombinant RT. (B) MS/MS fragmentation pattern for QNPDIVICQYMDDLYVGSDLEIGQHRW covalently modified with **I-7**. Peptides y4 to y15 were positively identified based on theoretical assignments in the MS spectrum (Supplementary Table S3).

illustrated in the figure, **I-7** cannot maintain an active conformation due to the loss of hydrogen bonds with Lys101, in agreement with its poor inhibitory activity of WT HIV-1 RT in enzymatic assays.

3. Conclusions

How to overcome drug resistance has always been one of the great challenges in clinical treatment of HIV-1. In this paper, we reported the design, synthesis and biological evaluation of a novel series of indolylarylsulfones as selective HIV-1 Y181C RT inhibitors, among which **I-7** and **I-9** demonstrated higher selectivity against mutant Y181C RT than against the WT HIV-1_{BH10} RT. Mass spectrometry determinations were consistent with the covalent modification of Y181C RT in the NNRTI binding site of p66. However, experimental evidence reveals the presence of additional targets in the RT, if the concentration of **I-7** is increased. The poor selectivity of the reaction under these conditions could explain the high cytotoxicity observed with most of the synthesized compounds, attributed to off-target labeling of viral and cellular proteins. However, our results indicated that selective labeling can be achieved by controlling the incubation time of the reaction and concentration of the covalent agent. Future efforts should be focused on avoiding off-target inhibition, probably by using reactive groups (warheads) with lower activity.

4. Experimental section

4.1. Chemistry

Mass spectrometry was performed on an API 4000 triple quadrupole mass spectrometer (Applied Biosystems/MDS Sciex, Concord, ON, Canada). ^{1}H NMR and ^{13}C NMR spectra were recorded on a Bruker AV-400 spectrometer (Bruker BioSpin, Switzerland), using solvents as indicated (DMSO-d_6). Chemical shifts were reported in δ values (ppm) with tetramethylsilane as the internal reference, and J values were reported in hertz (Hz). Melting points (mp) were determined on a micromelting point apparatus (Tian Jin Analytical Instrument Factory, Nankai, Tianjin, China). Flash column chromatography was performed on columns packed with silica gel 60 (200–300 mesh) (Qingdao waves silica gel desiccant co., Ltd, Qingdao, China). Thin layer chromatography was performed on pre-coated HUANGHAI® HSGF254, 0.15–0.2 mm TLC-plates (Yantai Jiangyou Silica Gel Development Co., Ltd., Yantai, Shandong, China). The key reactants were purchased from Bide Pharmatech Co. Ltd.

4.1.1. *Ethyl 5-bromo-3-(chlorosulfonyl)-1H-indole-2-carboxylate (3)*

Synthesis was initiated by adding acetic anhydride (28 mL) to the starting material **(1)** (7 g, 0.026 mol) at room temperature. The reaction mixture was subsequently cooled to 0 °C, and sulphuric acid (7 mL) was added drop wise. The reaction was stirred for 12–15 h at room temperature to ensure consumption of starting material. The solid was then filtered by suction filtration to get crude compound 5-bromo-2-

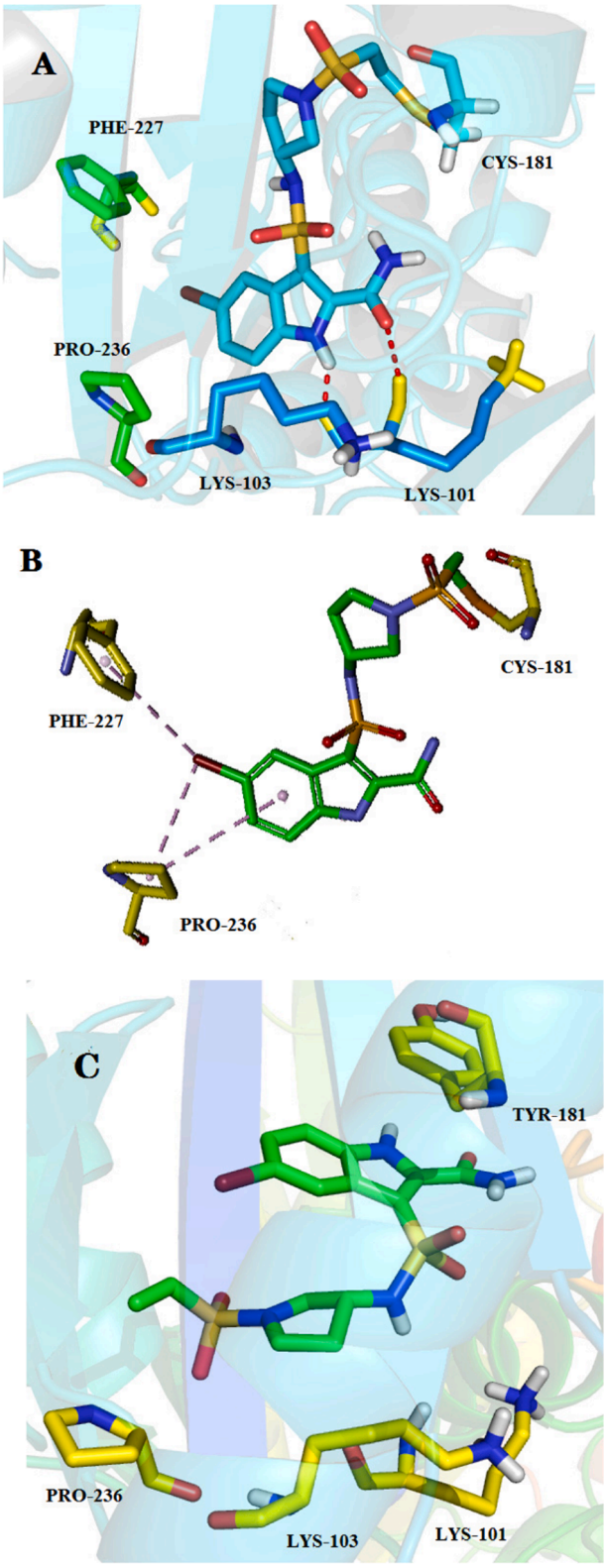

Fig. 6. Predicted binding modes of **I-7** in the NNRTI binding pocket of HIV-1 RT. (A, B) Docking of **I-7** in the allosteric site of HIV-1 Y181C RT (PDB code: 3DRR) using Discovery Studio 3.5, showing hydrogen bonds (dashed lines in red) with the polypeptide backbone of Lys101 (A) and additional interactions with the side chains of Phe227 and Pro236 (B). (C) Docking of **I-7** in the allosteric site of HIV-1 WT RT (PDB code: 2RF2) using Sybyl-X 2.0. Non-polar hydrogen atoms are omitted for clarity.

(ethoxycarbonyl)-1H-indole-3-sulfonic acid (**2**), which was taken to the next step without further purification.

Compound **2** (8 g, 0.023 mol) was suspended in dichloromethane (110 mL) to which catalytic amount of DMF (3.6 mL) was added and the mixture was stirred at room temperature till a clear solution was obtained. Oxalyl chloride (9.8 mL) in dichloromethane (50 mL) was added to the reaction mixture drop wise over a period of 15–20 min at room temperature. The reaction mixture was heated at 40 °C with stirring for 2–3 h. After evaporating a portion of dichloromethane, the reaction mixture is cooled to 0–5 °C and maintained for 1–1.5 h. The crude compound obtained was filtered, washed with chilled dichloromethane (40 mL) and dried at 40–45 °C to give compound **3** as a white solid. Yield 41%, ESI-MS: *m/z* 365.3 (M+1), 367.3 (M+1), $C_{11}H_9BrClNO_4S$ (366.62).

4.1.2. Synthesis of intermediate *4*

To a solution of ethyl 5-bromo-3-(chlorosulfonyl)-1H-indole-2-carboxylate (Compound 3, 2.5 g, 6.8 mmol) in dichloromethane (40 mL), triethylamine (1.9 mL) and alkylamine (7.5 mmol) were added successively at 0℃. The reaction was then stirred overnight at room temperature. On completion of the reaction, the reaction was quenched with water and the mixture was extracted with dichloromethane. The organic phase was shaken with saturated solution of sodium hydrogen carbonate and then brine, dried over anhydrous $MgSO_4$, filtered and concentrated under reduced pressure. Purification on silica gel (ethyl acetate: petroleum (EA:PE) = 1:3) gave intermediate **4** as a white solid.

(R)-ethyl-5-bromo-3-((3-((tert-butoxycarbonyl)amino)pyrrolidin-1-yl) sulfonyl)-1H-indole-2-carboxylate (***4–1***): white solid, yield: 39%. mp: 183–185 °C. ^{1}H NMR (400 MHz, DMSO-d_6) δ: 13.09 (s, 1H), 8.14 (d, J = 1.2 Hz, 1H), 7.55 (d, J = 8.5 Hz, 1H), 7.51 (d, J = 8.8 Hz, 1H), 7.00 (d, J = 6.1 Hz, 1H), 4.40 (q, J = 7.1 Hz, 2H), 3.89–3.85 (m, 1H), 3.51–3.38 (m, 2H), 3.33–3.27 (m, 1H), 3.14–3.11 (m, 1H), 1.94 (td, J = 13.8, 7.1 Hz, 1H), 1.66 (td, J = 13.2, 6.2 Hz, 1H), 1.36 (t, J = 7.1 Hz, 3H), 1.32 (s, 9H).^{13}C NMR (100 MHz, DMSO-d_6) δ: 159.89, 155.54, 133.84, 130.55, 128.44, 127.72, 123.92, 115.73, 112.58, 78.39, 62.57, 53.37, 50.21, 46.50, 30.73, 28.58, 14.32. ESI-MS: *m/z* 518.5 (M+H), 533.4 (M+NH_3), 535.3 (M+NH_3), 540.5 (M+Na), $C_{20}H_{26}BrN_3O_6S$ (516.41).

Ethyl-5-bromo-3-((4-((tert-butoxycarbonyl)amino)piperidin-1-yl)sulfonyl)-1H-indol-2-carboxylate (***4–3***): White solid, yield: 45%. mp: 229–231 °C. ^{1}H NMR (400 MHz, DMSO-d_6) δ:12.97 (s, 1H), 8.25 (s, 1H), 7.52 (s, 2H), 7.27 (d, J = 7.6 Hz, 1H), 4.45 (q, J = 7.1 Hz, 2H), 3.71 (d, J = 13.2 Hz, 2H), 3.31–3.27 (m,1H), 2.72 (d, J = 6.9 Hz, 2H), 1.57–1.53 (m, 2H), 1.38 (t, J = 7.1 Hz, 3H), 1.35 (s, 9H), 1.31–1.21(m, 2H). ESI-MS: *m/z* 532.5 (M+H), 549.5 (M+NH_3), 552.5 (M+Na), $C_{21}H_{28}BrN_3O_6S$ (530.43).

(R)-ethyl-5-bromo-3-(N-(1-(tert-butoxycarbonyl)piperidin-3-yl)sulfamoyl)-1H-indole-2-carboxylate (***4–4***): White solid, yield: 35%. mp: 185–187 °C. ^{1}H NMR (400 MHz, DMSO-d_6) δ: 13.03 (s, 1H), 8.24 (s, 1H), 7.52 (s, 2H), 7.30 (d, J = 7.6 Hz, 1H), 4.43 (q, J = 7.1 Hz, 2H), 3.67 (d, J = 12.8 Hz, 1H), 3.59 (d, J = 11.3 Hz, 1H), 3.13 (s, 1H), 2.66 (d, J = 13.4 Hz, 2H), 1.63 (s, 1H), 1.53 (d, J = 13.0 Hz, 1H), 1.37 (t, J = 7.1 Hz, 3H), 1.24 (s, 9H). ^{13}C NMR (100 MHz, DMSO-d_6) δ: 160.14, 154.14, 133.83, 128.84, 128.59, 126.65, 123.86, 117.89, 115.75, 115.60, 79.10, 62.61, 49.84, 31.00, 28.31, 23.80, 14.46. ESI-MS: *m/z* 530.3 (M+H), 532.3 (M+H), 552.4 (M+Na), 554.1 (M+Na), $C_{21}H_{28}BrN_3O_6S$ (530.43). *(S)-ethyl-5-bromo-3-(N-(1-(tert-butoxycarbonyl)pyrrolidin-3-yl)sulfamoyl)-1H-indole-2-carboxylate(**4–5**)*: White solid, yield:43%. mp: 118–120 °C. ESI-MS: *m/z* 516.5 (M+H), 535.3 (M+NH_3), 540.4 (M+Na), $C_{20}H_{26}BrN_3O_6S$ (516.41).

4.1.3. Synthesis of intermediate *5*

Intermediate **4** (0.2 g) was dissolved in a saturated solution of ammonia in methanol (10 mL) in a sealed tube at 70 °C overnight. After cooling, the reaction mixture was poured on ice water, stirred for 15 min, and extracted with ethyl acetate. The organic layer was washed with brine and dried and the solvent evaporated to afford a residue

which was purified on silica gel column chromatography (methanol-dichloromethane1:30 as eluent) to give intermediate **5**.

*(R)-tert-butyl-(1-((5-bromo-2-carbamoyl-1H-indol-3-yl)sulfonyl)pyrrolidin-3-yl)carbamate (**5–1**)*:White powder, yield:77%, mp: 210–211 °C. ^{1}H NMR (400 MHz, DMSO-d_6) δ: 12.92 (s, 1H), 8.37 (s, 1H), 8.21 (s, 1H), 8.09 (d, J = 1.5 Hz, 1H), 7.53–7.45 (m, 2H), 7.02 (d, J = 6.1 Hz, 1H), 3.87 (d, J = 5.6 Hz, 1H), 3.36 (d, J = 9.4 Hz, 1H), 3.31–3.27 (m, 1H), 3.22–3.20 (m, 1H), 2.99–2.95 (m, 1H), 1.92 (td, J = 13.8, 7.1 Hz, 1H), 1.63 (td, J = 13.0, 6.1 Hz, 1H), 1.32 (s, 9H). ^{13}C NMR (100 MHz, DMSO-d_6) δ: 160.99, 155.49, 135.71, 133.29, 127.89, 127.72, 123.42, 115.58, 115.44, 107.31, 78.45, 53.30, 49.07, 46.46, 30.69, 28.59. ESI-MS: *m/z* 511.0 (M+Na), $C_{18}H_{23}BrN_4O_5S$ (487.37).

*(R)-tert-butyl-3-(5-bromo-2-carbamoyl-1H-indole-3-sulfonamido)pyrrolidine-1-carboxylate (**5–2**)*: White solid, yield: 78%, mp: 121–123 °C. ^{1}H NMR (400 MHz, DMSO-d_6) δ: 12.76 (s, 1H), 8.39 (s, 1H), 8.20 (s, 1H), 8.16 (s, 1H), 8.05 (d, J = 6.7 Hz, 1H), 7.52–7.45 (m, 2H), 3.74–3.72 (m, 1H), 3.72–3.17 (m,2H), 3.14–3.07 (m, 1H), 2.94–2.87 (m, 1H), 1.89–1.81 (m, 1H), 1.73–1.60 (m, 1H), 1.3 (s, 9H). ^{13}C NMR (100 MHz, DMSO-d_6) δ: 161.11, 153.73, 134.91, 133.27, 127.69, 126.68, 123.43, 115.43, 115.19, 112.26, 78.75, 52.57, 49.07, 43.75, 30.91, 28.51. ESI-MS: *m/z* 409.1 (M+Na), 511.1 (M+Na), $C_{18}H_{23}BrN_4O_5S$ (487.37).

*tert-butyl-(1-((5-bromo-2-carbamoyl-1H-indol-3-yl)sulfonyl)piperidin-4-yl)carbamate (**5–3**)*: White solid, yield: 82%, mp: 242–244 °C. ^{1}H NMR (400 MHz, DMSO-d_6) δ:12.94 (s, 1H), 8.28 (s, 1H), 8.20 (s, 1H), 8.04 (d, J = 1.5 Hz, 1H), 7.53–7.46 (m, 2H), 6.84 (d, J = 7.2 Hz, 1H), 3.48–3.45 (m, 2H), 3.25 (d, J = 6.5 Hz, 1H), 2.59–3.54 (m, 2H), 1.76 (d, J = 10.4 Hz, 2H), 1.45–1.39 (m, 2H), 1.34 (s, 9H). ^{13}C NMR (100 MHz, DMSO-d_6) δ: 160.95, 155.24, 135.97, 133.31, 127.71, 127.54, 123.35, 115.62, 115.44, 107.09, 78.08, 46.19, 44.73, 31.12, 28.67. ESI-MS: *m/z* 523.1 (M+Na), 525.1 (M+Na), $C_{19}H_{25}BrN_4O_5S$ (501.39).

*(R)-tert-butyl-3-(5-bromo-2-carbamoyl-1H-indole-3-sulfonamido)piperidine-1-carboxylate (**5–4**)*:White solid, yield:99%, mp: 107–109 °C. ^{1}H NMR (400 MHz, DMSO-d_6) δ:12.70 (s, 1H), 8.38 (s, 1H), 8.19 (s, 1H), 8.18 (s, 1H), 7.94 (d, J = 6.7 Hz, 1H), 7.51–7.44 (m, 2H), 3.57 (d, J = 13.3 Hz, 2H), 2.99 (s, 1H), 2.69–2.63 (m, 2H), 1.60–1.52 (m, 2H), 1.27 (s, 9H), 1.17 (t, J = 7.1 Hz, 2H). ^{13}C NMR (100 MHz, DMSO-d_6) δ: 161.07, 154.15, 134.19, 133.25, 127.67, 126.90, 123.42, 115.50, 115.17, 113.24, 79.17, 60.22, 49.60, 49.07, 28.36, 21.23, 14.55. ESI-MS: *m/z* 523.1 (M+Na), 525.1 (M+Na), $C_{19}H_{25}BrN_4O_5S$ (501.39). *(S)-tert-butyl-3-(5-bromo-2-carbamoyl-1H-indole-3-sulfonamido)pyrrolidine-1-carboxylate (**5–5**)*:White solid, yield:88.3%, mp: 155–157 °C.

4.1.4. Synthesis of intermediate **6**

Trifluoroacetic acid (1 mL) was added dropwise under stirring to a solution of intermediate E (0.5 g) in CH_2Cl_2 (4 mL) at room temperature and stirred for 4 h. To the reaction mixture was added water and neutralized with 2 N NaOH to pH 8, and the organic layer was separated and dried over anhydrous $MgSO_4$, filtered and concentrated under reduced pressure to give the crude product **6**.

*(R)-3-((3-aminopyrrolidin-1-yl)sulfonyl)-5-bromo-1H-indole-2-carboxamide (**6–1**)*: White solid, ESI-MS: *m/z* 387.0 (M+H), 389.0 (M+H), $C_{13}H_{15}BrN_4O_3S$ (387.25).

*(R)-5-bromo-3-(N-(pyrrolidin-3-yl)sulfamoyl)-1H-indole-2-carboxamide (**6–2**)*: Brown solid, ESI-MS: *m/z* 387.4 (M+H), 389.4(M+H), $C_{13}H_{15}BrN_4O_3S$ (387.25).

*(R)-5-bromo-3-(N-(piperidin-3-yl)sulfamoyl)-1H-indole-2-carboxamide (**6–4**)*: White solid, ESI-MS: *m/z* 401.0(M+H), 403.0(M+H), $C_{14}H_{17}BrN_4O_3S$ (401.28).

4.1.5. Synthesis of target compounds

A solution of the acryl chloride (0.13 g, 0.71 mmol) in tetrahydrofuran was slowly added to a mixture solution of acryl chloride (1.2 eq) and Et_3N (1.5 eq) in dry tetrahydrofuran at −20 °C. The mixture was stirred at room temperature until the raw materials are consumed by TLC detection. The solvent was removed under reduced pressure, and the residue was purified by column chromatography on silica gel using methanol-dichloromethane 1:30 as eluent to give target compound.

4.1.5.1. *(R)-3-((3-acrylamidopyrrolidin-1-yl)sulfonyl)-5-bromo-1H-indole-2-carboxamide (**I-1**)*.

White crystal, yield: 42%. mp: 216–217 °C. ^{1}H NMR (400 MHz, DMSO-d_6) δ: 12.94 (s, 1H), 8.37 (s, 1H), 8.23 (s, 1H), 8.22 (s, 1H), 8.08 (d, J = 1.5 Hz, 1H), 7.53–7.45 (m, 2H), 6.05–6.03 (m, 2H), 5.54 (dd, J = 8.7, 3.6 Hz, 1H), 4.20–4.12 (m, 1H), 3.38–3.34 (m, 2H), 3.24–3.18 (m, 1H), 3.07–3.04 (m, 1H), 2.01 (td, J = 13.8, 7.1 Hz, 1H), 1.69 (td, J = 13.1, 6.7 Hz, 1H). ^{13}C NMR (100 MHz, DMSO-d_6) δ: 164.90, 161.03, 135.86, 133.28, 131.56, 127.85, 127.74, 125.96, 123.38, 115.59, 115.50, 107.13, 49.07, 48.91, 46.49, 30.74. ESI-MS: *m/z* 441.4 (M+H), 443.5 (M+H), 458.4 (M+NH_3), 460.4 (M+NH_3), 465.3 (M+Na), $C_{16}H_{17}BrN_4O_4S$ (441.30).

4.1.5.2. *(R)-3-(N-(1-acryloylpyrrolidin-3-yl)sulfamoyl)-5-bromo-1H-indole-2-carboxamide (**I-2**)*.

White crystal, yield: 34%. mp: 240–242 °C. ^{1}H NMR (400 MHz, DMSO-d_6) δ: 12.77 (s, 1H), 8.39 (s, 1H), 8.20 (s, 1H), 8.16 (s, 1H), 8.09 (dd, J = 11.7, 6.4 Hz, 1H), 7.53–7.45 (m, 2H), 6.53–6.31(m, 1H), 6.10–6.05 (m, 1H), 5.65–5.58 (m, 1H), 3.85–3.74 (m, 1H), 3.62–3.53 (m, 1H), 3.49–3.35 (m, 1H), 3.32–3.25 (m, 1H), 3.23–3.12 (m, 1H), 1.99–1.61 (m, 2H). ^{13}C NMR (100 MHz, DMSO-d_6) δ: 163.92, 161.13, 134.99, 133.29, 129.80, 129.57, 127.65, 127.25, 126.69, 123.42, 115.20, 112.14, 51.82, 51.28, 44.39, 31.97. ESI-MS: *m/z* 441.3 (M+H), 443.3 (M+H), 463.4(M+Na), 465.3 (M+Na), $C_{16}H_{17}BrN_4O_4S$ (441.30).

4.1.5.3. *3-((4-acrylamidopiperidin-1-yl)sulfonyl)-5-bromo-1H-indole-2-carboxamide (**I-3**)*.

White crystal, yield: 43%. Decompose at 267 °C. ^{1}H NMR (400 MHz, DMSO-d_6) δ: 12.95 (s, 1H), 8.28 (s, 1H), 8.20 (s, 1H), 8.05 (s, 1H), 8.02 (d, J = 7.3 Hz, 1H), 7.54–7.46 (m, 2H), 6.15 (dd, J = 16.9, 10.0 Hz, 1H), 6.03 (d, J = 16.8 Hz, 1H), 5.54 (d, J = 9.9 Hz, 1H), 3.62 (d, J = 6.7 Hz, 1H), 3.51 (d, J = 11.8 Hz, 2H), 2.63 (t, J = 10.7 Hz, 2H), 1.82 (d, J = 10.9 Hz, 2H), 1.43 (dd, J = 19.8, 9.5 Hz, 2H). ^{13}C NMR (100 MHz, DMSO-d_6) δ: 164.28, 160.99, 136.10, 133.33, 132.14, 127.71, 127.50, 125.63, 123.31, 115.63, 115.47, 107.11, 44.99, 44.78, 30.89. ESI-MS: *m/z* 455.3 (M+H), 457.3 (M+H), $C_{17}H_{19}BrN_4O_4S$ (455.33).

4.1.5.4. *(R)-3-(N-(1-acryloylpiperidin-3-yl)sulfamoyl)-5-bromo-1H-indole-2-carboxamide (**I-4**)*.

White crystal, yield: 35%. mp: 109–111 °C. ^{1}H NMR (400 MHz, DMSO-d_6) δ: 12.71 (s, 1H), 8.38 (s, 1H), 8.17 (s, 2H), 7.99 (d, J = 7.4 Hz, 1H), 7.51–7.44 (m, 2H), 6.22 (dd, J = 16.6, 10.4 Hz, 1H), 5.98 (dd, J = 45.5, 16.8 Hz, 1H), 5.56 (dd, J = 45.6, 10.3 Hz, 1H), 3.72 (d, J = 13.1 Hz, 1H), 3.53 (d, J = 11.6 Hz, 1H), 3.11–3.05 (m, 1H), 3.03–2.93 (m, 1H), 2.46–2.27 (m, 1H), 1.61–1.58 (m, 2H), 1.25 (td, J = 18.6, 10.4 Hz, 2H). ^{13}C NMR (100 MHz, DMSO-d_6) δ: 164.83, 161.20, 134.83, 133.24, 128.92, 128.37, 127.74, 126.69, 123.39, 115.45, 115.17, 51.69, 50.96, 49.91, 41.72, 30.80. ESI-MS: *m/z*456.99 (M+H), 489.02 (M+Na), $C_{17}H_{19}BrN_4O_4S$ (455.33).

4.1.5.5. *(S)-3-(N-(1-acryloylpyrrolidin-3-yl)sulfamoyl)-5-bromo-1H-indole-2-carboxamide (**I-5**)*.

White crystal, yield: 45%. mp: 217–218 °C. ^{1}H NMR (400 MHz, DMSO-d_6) δ: 12.80 (s, 1H), 8.40 (s, 1H), 8.21 (s, 1H), 8.16 (s, 1H), 8.09 (dd, J = 11.6, 6.4 Hz, 1H), 7.52–7.45 (m, 2H), 6.53–6.31 (m, 1H), 6.10–6.04 (m, 1H), 5.65–5.59 (m, 1H), 3.85–3.74 (m, 1H), 3.62–3.53 (m, 1H), 3.48–3.38 (m, 1H), 3.32–3.25 (m, 1H), 3.16–3.06 (m, 1H), 1.99–1.61 (m, 2H). ^{13}C NMR (100 MHz, DMSO-d_6) δ: 163.70, 161.14, 134.99, 133.30, 129.80, 129.57, 127.69, 127.27, 126.67, 123.42, 115.20, 112.14, 51.82, 51.28, 31.96. ESI-MS: *m/z* 441.3 (M+H), 463.3 (M+Na), 465.1 (M+Na), $C_{16}H_{17}BrN_4O_4S$ (441.30).

4.1.5.6. *(R)-5-bromo-3-((3-(vinylsulfonamido)pyrrolidin-1-yl)sulfonyl)-1H-indole-2-carboxamide (**I-6**)*.

White crystal, yield: 43%. mp: 217–218 °C. ^{1}H NMR (400 MHz, DMSO-d_6) δ: 13.02 (s, 1H), 8.41 (s, 1H), 8.29 (s, 1H), 8.14 (t, J = 4.1 Hz, 1H), 7.68 (d, J = 6.7 Hz, 1H), 7.58–7.51

(m, 2H), 6.70 (dd, J = 16.5, 9.9 Hz, 1H), 6.02 (d, J = 16.5 Hz, 1H), 5.98 (d, J = 9.9 Hz, 1H), 3.69–3.61 (m, 1H), 3.52–3.47 (m, 1H), 3.35–3.33 (m, 1H), 3.26–3.20 (m, 1H), 3.07–3.03 (m, 1H), 2.08–1.99 (m, 1H), 1.72 (td, J = 14.0, 7.1 Hz, 1H). ^{13}C NMR (100 MHz, DMSO-d_6) δ: 161.10, 137.57, 136.03, 133.29, 127.81, 127.71, 126.26, 123.34, 115.59, 115.47, 107.20, 53.27, 52.07, 46.14, 31.55. ESI-MS: m/z 478.94 (M+H), 500.92 (M+Na), $C_{15}H_{17}BrN_4O_5S_2$ (477.35).

4.1.5.7. (R)-5-bromo-3-(N-(1-(vinylsulfonyl)pyrrolidin-3-yl)sulfamoyl)-1H-indole-2-carboxamide ***(I-7)***. White crystal, yield: 37%. mp: 240–242 °C. ^{1}H NMR (400 MHz, DMSO-d_6) δ: 12.78 (s, 1H), 8.35 (s, 1H), 8.20 (s, 1H), 8.13 (s, 1H), 8.05 (d, J = 6.3 Hz, 1H), 7.54–7.45 (m, 2H), 6.76 (dd, J = 16.5, 10.0 Hz, 1H), 6.06 (d, J = 10.0 Hz, 1H), 6.01 (d, J = 16.5 Hz, 1H), 3.73 (dd, J = 12.3, 6.2 Hz, 1H), 3.22–3.16 (m, 2H), 3.13–3.07 (m, 1H), 2.90 (dd, J = 10.6, 5.5 Hz, 1H), 1.89 (td, J = 13.1, 6.4 Hz, 1H), 1.68 (td, J = 13.9, 7.0 Hz, 1H). ^{13}C NMR (100 MHz, DMSO-d_6) δ: 161.27, 135.46, 133.30, 132.03, 129.07, 127.66, 126.53, 123.34, 115.44, 115.21, 111.73, 52.81, 52.37, 46.04, 31.54. ESI-MS: m/z 477.0 (M+H), 479.0 (M+H), 499.0 (M+Na), 501.0 (M+Na), $C_{15}H_{17}BrN_4O_5S_2$ (477.35).

4.1.5.8. 5-bromo-3-((4-(vinylsulfonamido)piperidin-1-yl)sulfonyl)-1H-indole-2-carboxamide ***(I-8)***. White crystal, yield: 33%. mp: 269–270 °C. ^{1}H NMR (400 MHz, DMSO-d_6) δ: 12.97 (s, 1H), 9.35 (d, J = 7.6 Hz, 1H), 8.28 (s, 1H), 8.21 (s, 1H), 8.04 (s, 1H), 7.53–7.46 (m, 2H), 6.68 (dd, J = 16.5, 9.9 Hz, 1H), 5.96 (d, J = 16.5 Hz, 1H), 5.87 (d, J = 9.9 Hz, 1H), 3.64 (d, J = 12.1 Hz, 2H), 3.44–3.40 (m, 1H), 3.08–3.02 (m, 1H), 2.62–2.55 (m, 1H), 1.81 (d, J = 12.7 Hz, 2H), 1.59–1.45 (m, 2H). ESI-MS: m/z 493.0 (M+H), 513.0 (M+Na), $C_{16}H_{19}BrN_4O_5S_2$ (491.38).

4.1.5.9. (R)-5-bromo-3-(N-(1-(vinylsulfonyl)piperidin-3-yl)sulfamoyl)-1H-indole-2-carboxamide ***(I-9)***. White crystal, yield: 36%. mp: 130–132 °C. ^{1}H NMR (400 MHz, DMSO-d_6) δ: 12.74 (s, 1H), 8.37 (s, 1H), 8.21 (s, 1H), 8.16 (s, 1H), 8.01 (d, J = 7.6 Hz, 1H), 7.52–7.45 (m, 2H), 6.72 (dd, J = 16.5, 10.0 Hz, 1H), 6.06 (d, J = 10.0 Hz, 1H), 5.98 (d, J = 16.5 Hz, 1H), 3.30 (d, J = 4.0 Hz, 1H), 3.25–3.20 (m, 2H), 2.62–2.56 (m, 1H), 2.48–2.45 (m, 1H), 1.65–1.61 (m, 1H), 1.51–1.47 (m, 1H), 1.35–1.29 (m, 1H), 1.22–1.13 (m, 1H). ^{13}C NMR (100 MHz, DMSO-d_6) δ: 161.12, 134.61, 133.81, 133.22, 129.19, 127.71, 126.70, 123.37, 115.46, 115.21, 112.91, 50.76, 49.23, 45.32, 30.08, 23.31. ESI-MS: m/z 492.95 (M+H), 514.93 (M+Na), $C_{16}H_{19}BrN_4O_5S_2$ (491.38). ^{13}C NMR (100 MHz, DMSO-d_6) δ: 161.27, 135.46, 133.30, 132.03, 129.07, 127.66, 126.53, 123.34, 115.44, 115.21, 111.73, 52.81, 52.37, 46.04, 31.54. ESI-MS: m/z 477.0 (M+H), 479.0 (M+H), 499.0 (M+Na), 501.0 (M+Na), $C_{15}H_{17}BrN_4O_5S_2$ (477.35).

4.1.6. Stability assays

Approximately 1 mg of **I-7** was weighed and dissolved in DMSO to obtain a 50 mM solution of the compound, and then diluted to a final concentration of 2.5 mM in commercial 0.1 M phosphate buffer solutions at pH 2.0 and 7.4 (Beijing Leagene Biotechnology, China). After incubating the sample for 24 h at room temperatures, the stability of the compound was tested by measuring the retention time and peak recovery by reverse-phase HPLC using an Inertsil ODS-3 column (GL Sciences, Tokyo, Japan), and a methanol/water mobile phase.

4.1.7. Reference NNRTIs

Efavirenz was obtained from the AIDS Research and Reference Reagent Program, Division of AIDS, NIAID, NIH. Etravirine and rilpivirine were supplied by Tibotec Pharmaceuticals, Inc. L-737,126 was synthesized as previously described.[13,14] Compound 7e was obtained by using methods described above. NMR parameters for this compound were: ^{1}H NMR (400 MHz, DMSO-d_6) δ 12.92 (s, 1H), 8.31 (d, J = 63.8 Hz, 2H), 8.12 (d, J = 1.8 Hz, 1H), 7.52 (d, J = 8.8 Hz, 1H), 7.47 (dt, J = 8.7, 1.4 Hz, 1H), 3.15–3.18 (m, 4H), 1.76 – 1.54 (m, 4H); ^{13}C NMR (100 MHz, DMSO-d_6) δ 161.06, 135.59, 133.25, 127.86, 127.72, 123.46, 115.58, 115.39, 107.62, 47.95(2 × C), 25.01(2 × C).

4.2. In vitro anti-HIV assays

Evaluation of the antiviral activity of the compounds against HIV in MT-4 cells was performed using the MTT assay as previously described.[15,16] Stock solutions (10 × final concentration) of test compounds were added in 25 µl volumes to two series of triplicate wells so as to allow simultaneous evaluation of their effects on mock- and HIV-infected cells at the beginning of each experiment. Serial 5-fold dilutions of test compounds were made directly in flat-bottomed 96-well microtiter trays using a Biomek 3000 robot (Beckman instruments, Fullerton, CA). Untreated HIV- and mock-infected cell samples were included as controls. HIV stock (50 µl) at 100–300 $CCID_{50}$ (50% cell culture infectious doses) or culture medium was added to either the infected or mock-infected wells of the microtiter tray. Mock-infected cells were used to evaluate the effects of test compound on uninfected cells in order to assess the cytotoxicity of the test compounds. Exponentially growing MT-4 cells were centrifuged for 5 min at 220 g and the supernatant was discarded. The MT-4 cells were resuspended at 6 × 10^5 cells/ml and 50 µl volumes were transferred to the microtiter tray wells. Five days after infection, the viability of mock-and HIV-infected cells was examined spectrophotometrically using the MTT assay. The MTT assay is based on the reduction of yellow colored 3-(4,5-dimethylthiazol-2-yl)-2,5-diphenyltetrazolium bromide (MTT) (Acros Organics) by mitochondrial dehydrogenase activity in metabolically active cells to a blue-purple formazan that can be measured spectrophotometrically. The absorbances were read in an eight-channel computer-controlled photometer (Infinite M1000, Tecan), at two wavelengths (540 and 690 nm). All data were calculated using the median absorbance value of three wells. The 50% cytotoxic concentration (CC_{50}) was defined as the concentration of the test compound that reduced the absorbance (optical density at 540 nm) of the mock-infected control sample by 50%. The concentration achieving 50% protection against the cytopathic effect of the virus in infected cells was defined as the 50% effective concentration (EC_{50}).

4.3. Nucleotide incorporation and RT DNA polymerase inhibition assays

WT HIV-1_{BH10} RT was expressed in *E. coli* and purified as previously described.[17,18] Inhibition of the DNA polymerase activity was determined in single nucleotide incorporation assays carried out with template-primer D38/25PGA, essentially as previously described.[19] Synthetic oligonucleotides D38 (5'-GGGTCCTTTCTTACCTGCAA-GAATGTATAGCCCTACCA-3') and 25PGA (5'-TGGTAGGGCTATA-CATTCTTGCAGG-3') were obtained from Sigma-Aldrich. The primer 25PGA was labeled at its 5' terminus with 1–2 µCi of [γ-^{32}P]ATP (10 mCi/ml; 3000 Ci/mmol, Perkin Elmer) and 5 units of T4 polynucleotide kinase (New England Biolabs) in 70 mM Tris-HCl pH 7.6 buffer, containing 10 mM $MgCl_2$ and 5 mM DTT. In some experiments, DTT was excluded from the reaction mixture. The labeled primer was then annealed to D38 in 150 mM magnesium acetate and 150 mM NaCl. The template/primer molar ratio was adjusted to 1:1 and the concentration was 3 µM. Before the assay, the template-primer was diluted to a final concentration of 300 nM in 550 mM Hepes pH 7.0 buffer, containing 150 mM magnesium acetate and 150 mM NaCl.

Nucleotide incorporation reactions were carried out in 50 mM Hepes buffer pH 7.0, containing 15 mM magnesium acetate, 15 mM NaCl, 130 mM potassium acetate, 1 mM DTT and 5% polyethylene glycol 6000. The concentrations of WT HIV-1_{BH10} RT and D38/25PGA in these assays were 12 nM and 30 nM, respectively. RT, template-primer and varying concentrations of the inhibitors were incubated at 37 °C for 5 or 60 min, before initiating the reaction by adding dTTP (GE Healthcare) to a final concentration of 100 µM. As a control, efavirenz, L-737,126 and compound 7e were tested under the same conditions. Nucleotide incorporation reactions were incubated for 15 and 30 s and then terminated by

adding an equal volume of stop solution (10 mM EDTA in 90% formamide containing 1 mg/mL xylene cyanol FF and 1 mg/mL bromphenol blue). Results were visualized on denaturing 20% polyacrylamide-8 M urea gels and primer extensions were determined by phosphoroimaging with a BAS1500 scanner (Fuji), using the program Tina version 2.09 (Raytest Isotopenmessgerate Gmbh, Staubenhardt, Germany). IC_{50} values (μM) were obtained from dose-response curves using the GraphPad Prism software, after calculating the amount of elongated primer in the absence of inhibitor (at 5% DMSO) and in the presence of drug at concentrations in the range of 0.01–100 μM.

4.4. Mass spectrometry

Matrix-assisted laser desorption/ionization-time of flight (MALDI-TOF) mass spectrometry was used to determine the molecular weight of complexes of **I-7** with mutant Y181C HIV-1_{BH10} RT. The enzyme at a final concentration of 29.4 μM was incubated with the inhibitor (at different concentrations) in 50 mM Tris-HCl pH 8.0, containing 50 mM NaCl, 5 mM $MgCl_2$ and 3.3% DMSO at 37 °C during 60 min. Then, inhibitor and salts were removed by centrifugal ultrafiltration (10,000 molecular weight cut-off membranes, Microcon-10, Amicon, Merck Millipore). The sample (15 μl) was diluted 20-fold with ultrapure distilled water and centrifuged at 14,000*g* for 6 min. The process was repeated several times until the absorbance of the filtrate was below 0.001, in the range of 220–300 nm. The desalted protein was dried, resuspended in 30 μl of aqueous 2% trifluoroacetic acid (TFA) solution. Samples were diluted at 1:1 ratio (v/v) with matrix solution (50% saturated sinapinic acid in 70% aqueous acetonitrile and 0.1% trifluoroacetic acid). A 1.0 μl aliquot of this mixture was manually deposited onto a 386-well OptiTOFTM Plate (ABSciex, Foster City, CA) and allowed to dry at room temperature.

Molecular weights were determined by using an ABi 4800 MALDI TOF/TOF mass spectrometer (SCIEX, Foster City, CA) in positive ion linear mode (the ion acceleration voltage was 25 kV for MS acquisition). The detection mass range was set between 3000 and 90,000 *m/z*.

4.4.1. Trypsin digestion

Samples were diluted in 20 μl of multichaotropic sample solution UTT buffer (7 M urea, 2 M thiourea, 100 mM triethyl ammonium bicarbonate (TEAB) (Sigma-Aldrich)), reduced with 2 μl of 50 mM Tris(2-carboxyethyl)phosphine (TCEP), pH 8.0, at 37 °C for 60 min, followed by addition of 2 μl of 100 mM cysteine-blocking reagent chloroacetamide (Sigma-Aldrich) for 20 min at room temperature. Sample was diluted to 140 μl to reduce the urea concentration with 25 mM TEAB. Finally, digestion was initiated by adding 0.2 μg of Pierce MS-grade trypsin (Thermo-Fisher Scientific Inc.) to each sample in a ratio 1:20 (w/w), and then incubated at 37 °C overnight on a shaker. Sample digestion was evaporated to dryness in a vacuum concentrator and resuspended in 0.1% formic acid.

4.4.2. LC-ESI MS/Ms

A 1 μg aliquot of each digested sample was subjected to 1D-nano LC ESI-MS/MS analysis using a nano-liquid chromatography system (Eksigent Technologies nanoLC Ultra 1D plus, SCIEX, Foster City, CA) coupled to high speed Triple TOF 5600 mass spectrometer (SCIEX, Foster City, CA) with a Nanospray III source. Peptides were separated using a 40 min-gradient ranging from 2% to 90% mobile phase B (mobile phase A: 2% acetonitrile, 0.1% formic acid; mobile phase B: 100% acetonitrile, 0.1% formic acid). The eluent was further analyzed with a TripleTOF 5600 System (SCIEX, Foster City, CA) in a positive ion mode. Mass spectra were acquired over a range of 100–1800 *m/z*. The maximum ion injection time was set at 250 ms for the survey scan and 100 ms for MS/MS scans for the 35 most intense signals in the acquired mass spectra.

4.4.3. Analysis of peptides

MS/MS spectra were exported to mgf format and searched using Mascot Server 2.7.1 (Matrix Science) against a custom protein database, containing the amino acid sequence encoded within the *pol* gene of HIV-1 together with commonly occurring contaminants. Search parameters were set as follows: enzyme, trypsin; allowed missed cleavages, 2; carbamidomethyl (C) as fixed modification and acetyl (Protein *N*-term), pyrrolidone from E, pyrrolidone from Q and Oxidation (M) as variable modifications. Peptide mass tolerance was set to ±25 ppm for precursors and 0.05 Da for fragment masses.

4.5. Computational methods

Molecular docking of compound **I-7** was performed with the Tripos molecular modeling packages Sybyl-X 2.0,[20] and optimized for 2000-generations until the maximum derivative of energy became 0.005 kcal/(mol*A), using the Tripos force field. Atomic point charges were calculated using the Gasteiger-Huckel parameters. Docking analysis was carried out with the surflex-docking module of Discovery Studio 3.5, and the crystal structures of HIV-1 RT/NNRTI complexes (PDB files 2RF2 and 3DRR, for WT and mutant Y181C RTs). Bound ligands and water molecules were removed from the models. Then, hydrogen atoms were added, side chain amides and side chains bumps fixed, and charges and atom types were assigned according to CHARMM. After generating the protomol, the optimized **I-7** was docked into the NNRTI binding pocket, setting the relevant parameters as defaults. Top-scoring poses were determined with the Sybyl-X 2.0 software and shown by the software of PyMOL version 1.5 (www.pymol.org).

Declaration of Competing Interest

The authors declare that they have no known competing financial interests or personal relationships that could have appeared to influence the work reported in this paper.

Acknowledgments

Financial support from the National Natural Science Foundation of China (NSFC No. 81273354), the Key Project of NSFC for International Cooperation (No. 81420108027), the Key Research and Development Project of Shandong Province (No. 2017CXGC1401), the Young Scholars Program of Shandong University (YSPSDU No. 2016WLJH32, to P. Z.) and the Major Project of Science and Technology of Shandong Province (No. 2015ZDJS04001) are gratefully acknowledged. Work in Madrid was supported by grants PID2019-104176RB-I00/AEI/10.13039/501100011033) (Spanish Ministry of Science and Innovation) and 2019AEP001 (CSIC), as well as an institutional grant of Fundación Ramón Areces (awarded to the CBMSO). Protein and peptide identifications by MS-MALDI-TOF and LC-ESI MS/MS were carried out in the Proteomics Facility of the Spanish National Center for Biotechnology (CNB-CSIC) that belongs to ProteoRed, PRB3-ISCIII, supported by grant PT17/0019. The technical assistance of Kris Uyttersprot and Kristien Erven in antiviral assays and Sergio Ciordia and Carlos García in mass spectrometry are gratefully acknowledged. Authors also thank Dr. Francisco J. Corrales (CNB-CSIC) for helpful suggestions.

Appendix A. Supplementary material

Supplementary data to this article can be found online at https://doi.org/10.1016/j.bmc.2020.115927.

References

1 Zhan P, Pannecouque C, De Clercq E, Liu X. Anti-HIV drug discovery and development: current innovations and future trends. *J Med Chem*. 2016;59:2849–2878.

2 Gubernick SI, Felix N, Lee D, Xu JJ, Hamad B. The HIV therapy market. *Nat Rev Drug Discovery*. 2016;15:451–452.
3 Menéndez-Arias L. Molecular basis of human immunodeficiency virus type 1 drug resistance: overview and recent developments. *Antiviral Res*. 2013;98:93–120.
4 Lai MT, Munshi V, Lu M, et al. Mechanistic study of common non-nucleoside reverse transcriptase inhibitor-resistant mutations with K103N and Y181C substitutions. *Viruses*. 2016;8:263.
5 de Bethune MP. Non-nucleoside reverse transcriptase inhibitors (NNRTIs), their discovery, development, and use in the treatment of HIV-1 infection: a review of the last 20 years (1989–2009). *Antiviral Res*. 2010;85:75–90.
6 Rhee SY, Blanco JL, Jordan MR, et al. Geographic and temporal trends in the molecular epidemiology and genetic mechanisms of transmitted HIV-1 drug resistance: an individual-patient- and sequence-level meta-analysis. *PLoS Med*. 2015; 12:e1001810.
7 Avila-Rios S, Sued O, Rhee SY, Shafer RW, Reyes-Teran G, Ravasi G. Surveillance of HIV transmitted drug resistance in Latin America and the Caribbean: a systematic review and meta-analysis. *PLoS ONE*. 2016;11, e0158560.
8 Chan AH, Lee WG, Spasov KA, et al. Covalent inhibitors for eradication of drug-resistant HIV-1 reverse transcriptase: From design to protein crystallography. *PNAS*. 2017;114:9725–9730.
9 Williams TM, Ciccarone TM, MacTough SC, et al. 5-Chloro-3-(phenylsulfonyl)indole-2-carboxamide: a novel, non-nucleoside inhibitor of HIV-1 reverse transcriptase. *J Med Chem*. 1993;36:1291–1294.
10 Silvestri R, De Martino G, La Regina G, et al. Novel indolyl aryl sulfones active against HIV-1 carrying NNRTI resistance mutations: synthesis and SAR studies. *J Med Chem*. 2003;46:2482–2493.
11 Famiglini V, Silvestri R. Indolylarylsulfones, a fascinating story of highly potent human immunodeficiency virus type 1 non-nucleoside reverse transcriptase inhibitors. *Antiviral Chem Chemotherapy*. 2018;26, 2040206617753443.
12 Zhao Z, Wolkenberg SE, Sanderson PE, et al. Novel indole-3-sulfonamides as potent HIV non-nucleoside reverse transcriptase inhibitors (NNRTIs). *Bioorg Med Chem Lett*. 2008;18:554–559.
13 Zhao T, Meng Q, Kang D, et al. Discovery of novel indolylarylsulfones as potent HIV-1 NNRTIs via structure-guided scaffold morphing. *Eur J Med Chem*. 2019;15, 111619.
14 Li X, Gao P, Huang B, et al. Discovery of novel piperidine-substituted indolylarylsulfones as potent HIV NNRTIs via structure-guided scaffold morphing and fragment rearrangement. *Eur J Med Chem*. 2017;27:190–201.
15 Pauwels R, Balzarini J, Baba M, et al. Rapid and automated tetrazolium-based colorimetric assay for the detection of anti-HIV compounds. *J Virol Methods*. 1988; 20:309–321.
16 Pannecouque C, Daelemans D, De Clercq E. Tetrazolium-based colorimetric assay for the detection of HIV replication inhibitors: revisited 20 years later. *Nat Protoc*. 2008; 3:427–434.
17 Boretto J, Longhi S, Navarro JM, Selmi B, Sire J, Canard B. An integrated system to study multiply substituted human immunodeficiency virus type 1 reverse transcriptase. *Anal Biochem*. 2001;292:139–147.
18 Matamoros T, Deval J, Guerreiro C, Mulard L, Canard B, Menendez-Arias L. Suppression of multidrug-resistant HIV-1 reverse transcriptase primer unblocking activity by alpha-phosphate-modified thymidine analogues. *J Mol Biol*. 2005;349: 451–463.
19 Betancor G, Alvarez M, Marcelli B, Andres C, Martinez MA, Menendez-Arias L. Effects of HIV-1 reverse transcriptase connection subdomain mutations on polypurine tract removal and initiation of (+)-strand DNA synthesis. *Nucleic Acids Res*. 2015;43: 2259–2270.
20 Sybyl-X Molecular Modeling Software Packages, Version 2.0. TRIPOS Associates, Inc; St. Louis, MO, USA; 2012.